Available online at www.sciencedirect.com

ScienceDirect

Proceedings of the Combustion Institute 35 (2015) 3653-3661

ELSEVIER

CrossMark

Proceedings of the Combustion Institute

www.elsevier.com/locate/proci

Calibration-free, high-speed, in-cylinder laser absorption sensor for cycle-resolved, absolute H_2O measurements in a production IC engine

0. Witzel[a], A. Klein[a], C Meffert[b], C.Schulz[b], **S.A. Kaiser**[b], **V. Ebert**[a,c,*]

[a] *Physika/isch-Technische Bundesansta/t, PTB, Bundesallee 100, 38116 Braunschweig, Germany*

[b] *Institute for Combustion and Gas Dynamics - Reactive Fluids, IVG, University of Duisburg-Essen, 47048 Duisburg, Germany*

[c] *Center of Smart Interfaces, CS/, TU Darmstadt, Alarich-Weiss-Stra}Je IO, 64287 Dam1stadt, Germany*

Available online 27 June 2014

Abstract

The performance of a hygrometer based on calibration-free direct tunable diode laser absorption spectroscopy (dTDLAS) for in-cylinder H_2O measurements is demonstrated in a nearly unmodified production internal combustion engine. The H_2O concentration is a proxy for the residual gas fraction remaining in the cylinder after intake-valve closure. One challenge for in-cylinder measurements, especially in multi-cylinder engines, is to obtain optical access to the combustion chamber. The measurements here were performed in the flywheel-side cylinder of a four-cylinder engine with small access ports that were previously designed for endoscopic imaging. Due to their position these ports prohibit the usual collinear arrangement of the optical elements typical for line-of-sight measurement techniques. Therefore, we developed a new "angled" fiber-optical interface, which allows a trans-illumination of the engine at a 90° angle. The optical fiber interface uses a scattering target inside the combustion chamber with its 84 mm bore achieving an absorption length of about 70 mm. With this arrangement, crank-angle resolved measurements of the H_2O concentration during early compression could be realized with a temporal resolution of 250 µs and a H_2O detection limit of 0.074 vol.%. This allows detailed analysis of single engine cycles as needed for residual gas investigations. Measurements were performed over a range of loads (25--100 Nm) and speeds (1400-3650 rpm), over which the residual gas fraction was expected to vary significantly. H_2O concentrations were measured between 3.3 and 5.0 vol.%. The results werecompared with a simple model of residual gas content and were found to agree within the combined uncertainty of both methods, which gives an indication that dTDLAS can be used to validate more complex engine models beyond what is possible by pressure-trace analysis.

Keywords: IC engine; Residual gas; Spectroscopy; Tunable diode laser absorption; Combustion diagnostics

* Corresponding author. Fax: +49 531 592 3209.
E-mail address: volker.ebert@ptb.de (0. Witzel).

http://dx.doi.org/10.1016/j.proci.2014.06.038
1540-7489/

1. Introduction

Modern combustion strategies for internal combustion (IC) engines often use elevated levels of residual burnt gas (or short, residual gas) to reduce the flame temperature and therefore suppress the formation of nitrogen oxides (NO_x). Residual gas levels can be increased either by returning gas from the exhaust pipe to the intake (external exhaust-gas recirculation, **EGR)** or by purposely retaining burnt gas in the cylinder at the end of the exhaust stroke (internal **EGR).** However, if the residual gas concentration is too high, efficiency suffers and, depending on the level of cycle-to-cycle variability, misfires can ensue. Therefore, exact knowledge of the amount of residual gas before ignition is important in engine development. While the amount of residual gas provided by external EGR can be estimated with reasonable effort, no satisfying solution exists for the quantification of residual gas due to internal EGR. Current commercially available techniques like gas sampling and subsequent analysis with a gas chromatograph or mass spectrometer mostly yield cycle-averaged information (1,2]. In contrast, optical *in situ* methods offer a sampling-free cycle-resolved analysis with high temporal resolution.

To this end, several optical diagnostics have been applied in IC engines in the past, for example coherent anti-Stokes Raman spectroscopy (CARS) [3], laser-induced fluorescence (LIF) [4], infrared absorption spectroscopy [5--9] and Fourier-transform infrared spectroscopy (FTIR) (10]. Direct tunable-diode laser absorption spectroscopy (dTDLAS) allows the development of compact sensors needing only minimally-invasive optics to access the cylinder volume. The advantages of dTDLAS were discussed in detail in previous work (11,12]. Concentration measurements of several combustion-related species were performed in the past, *e.g.,* H_2O (11,13], CO (14], or CO_2 (15], with high temporal resolution (16]. With known fuel composition, both H_2O and CO_2 can be used as proxy species for residual gas. We already demonstrated a method of dTDLAS to determine the H_2O concentration without the need for calibration (17], which is a significant advantage due to the avoidance of complicated calibration strategies of previous methods. In dTDLAS, species concentration, background emission, and transmission losses can be directly inferred from the detector signal. Gas temperature and pressure are derived from simultaneous auxiliary measurements. The spectral line parameters are taken from spectral databases like **HITRAN** (18].

Current commercially available spectrometers using a spectrally broadband light source for residual gas measurements need calibration, *e.g.,* by installing an additional sensor to measure the engine's intake air humidity [19]. This calibration not only increases experimental effort and measurement uncertainty substantially but also complicates interpretation of the results.

Previously, we performed dTDLAS in an optically-accessible single-cylinder research engine to measure the H_2O concentration during the compression stroke in motored operation (11,12]. Subsequently, less invasive access through small ports in a metal liner was implemented and the pressure range was expanded by use of a different laser type [11,12]. Here we present, to our best knowledge, for the first time, global H_2O-concentration measurements with dTDLAS in a fired multi-cylinder production engine. The engine has been modified only very slightly to permit minimally-invasive access to one of the cylinders. We describe the hardware implementation and also compare the measurements to model-based estimates of the residual gas content for a range of operating points.

2. Experiments

The following section is divided into three subsections describing engine hardware, the principle of dTDLAS, and finally the fiber-optical interface developed here.

2.1. Engine

Measurements under fired engine conditions were performed in the flywheel-side cylinder of a BMW "N46 B20 AA" four-cylinder in-line engine with a total displacement of 1995 cm^3 (84 mm bore, 90 mm stroke, geometric compression ratio 1:10). Figure 1 shows a photograph of the engine head. In addition to the standard M14 spark-plug

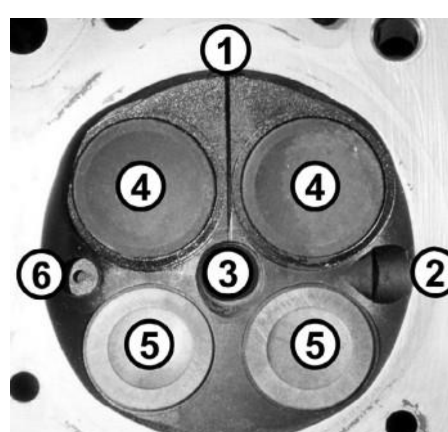

Fig. 1. The part of the engine head that was modified for the laser-based measurements. Labels: (1) laser-sheet input port (not used here), (2) endoscope port, (3) M14 spark-plug bore, (4) intake valves, (5) exhaust valves, and (6) M10 bore for additional sensors [22).

bore (label 3) the engine is equipped with access for an MIO pressure sensor (6) and a perpendicular arrangement for laser-sheet input (1) and endoscopic imaging (2) [20,21], both with 12 mm bore diameter. As shown in Fig. 1, due to their geometric arrangement with respect to each other, in general none of these ports are suitable for typical, collinear line-of-sight measurement using dTDLAS.

In this engine, load is not controlled by a conventional throttle, but by continuously variable valve lift and camshaft phasing (BMW "Valvetronic" and "VANOS"). The engine was controlled via the production engine control unit which allowed read-out access, but no active control. This prevented specific variations of the residual gas fraction, for example by varyingvalve timings. Therefore, load and speed sweeps (Table 1) were performed within the limits of the dynamometer in order to vary residual gas content and hence H_2O concentration. The exhaust-valve lift remained constant at 9.7 mm, while intake-valve lift and valve phasing were varied by the engine control unit as listed in Table 1, which shows that in general the engine control unit is tuned to increase both intake-valve lift and valve overlap with speed and load. At each operating point **(OP)**, the dTDLAS signal and the time-resolved pressure in the cylinder and its intake and exhaust were recorded for 50 consecutive cycles. The fuel was iso-octane, supplied by port fuel injection.

For the load sweep (OP 1-4), Fig. 2 shows the pressure (top) and the temperature trace (bottom). The latter was calculated by a three-pressure analysis **(TPA)**, a "quasi-dimensional" model implemented in GT-Power© [22]. Strictly speaking, residual gas content needs to be *known* for calculating the temperature during the compression stroke. In its temperature calculation, the TPA analysis *estimates* residual gas content, thereby resolving this interdependence, but the inherent assumptions and approximations introduce a potential error, which has been accounted for in the uncertainty analysis in Section 3.

Table I
Engine operating points **(OP)** including intake-valve lift **(IVL)** and (positive) valve overlap **(VO)**.

OP	Speed (rpm)	Load (Nm)	IVL (mm)	VO (CAD)
1	2100	25	I.I	71.5
2	2100	50	1.6	87.2
3	2100	75	2.2	93.8
4	2100	100	2.8	92.4
5	1400	50	1.3	80.7
6	1950	50	1.6	90.4
7	2900	50	2.3	93.2
8	3650	50	3.1	90.2

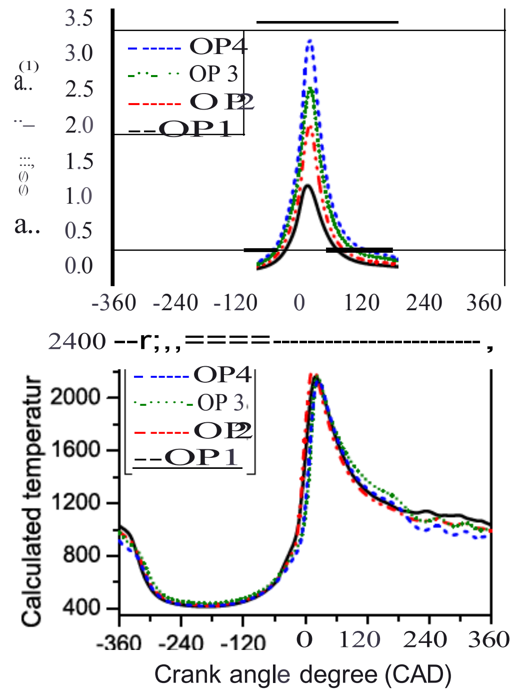

Fig. 2. Measured pressure and calculated temperature trace for OP 1-4.

The results of the **dTDLAS** measurements were compared to a simple zero-dimensional model, specifically developed [23] to calculate the residual gas fraction after intake-valve closure. The model does this in three steps. First, the residual gas mass at intake valve opening is calculated using the ideal-gas law with the volume given by piston kinematics. The second step considers the difference in residual gas mass due to the change of cylinder volume during valve overlap, *i.e.*, between intake valve opening and exhaust-valve closure, and the third part the difference due to the pressure difference between intake and exhaust. Input parameters for the model are the pressures in intake, cylinder, and exhaust, the exhaust temperature, and geometric engine parameters including valve flow-coefficients. This quite simple model was originally developed for real-time application in engine control units. Here, for the first time the possibility exists for a direct assessment of its performance byconverting residual gas content to H_2O concentration, which is measured by the dTDLAS sensor.

2.2. dTDLAS

dTDLAS is based on the wavelength-dependent attenuation of quasi-monochromatic light passing through a gas sample. The attenuation can be described by the extended Lambert-Beer law [24-26]with additional parameters taking into account background emission *E(t)* and broadband optical transmission losses *Tr(* t):

$$/(\mathrm{v})=\mathrm{lo}(\mathrm{v})\times Tr(t)\times e^{-S(T)xg(M.)xNxL}+E(t) \qquad (1)$$

with *N* being the number density of the molecular absorbers, $/_0(\mathrm{v})$ the initial laser intensity, $/_0(\mathrm{v})$ the intensity detected after the probe volume of absorption length *L* and the wavenumber ii in cm-1. The absorption-line profile is characterized by the area-normalized line shape function *g(v -* ii0), which is centered at the wavenumber vo, and the temperature-dependent, spectrally-integrated, line strength S(7).

Spectrally integrating the absorption line shape *g(v -* ii0) over the wavenumber V, solving Eq. (1) for the absorber density *N,* and using the ideal-gas law $N=p/k_8T$ (k_8: Boltzmann constant, *p:* pressure, *T:* temperature) leads to the species concentration *c:*

$$c=\frac{k_8\times T}{S(T)\times L\times p}\int\frac{/_0(\mathrm{ii})\times Tr(t)}{I(v)-E(t)}\,\frac{dv}{dt}\,dt \qquad (2)$$

Hence the concentration can be determined without the need for calibration, solely with knowledge of the line strength S(7), the experimental boundary conditions *(p, T, Tr(t),* E(t)) and the dynamic laser-tuning coefficient *dv/dt).* Adetailed description of the method can be found in [24-26].

The opto-electronics consist of a distributed feedback **(DFB)** diode laser, temperature-stabilized by a Peltier element and coupled into a single-mode fiber. A function generator provided a periodic triangular signal modulating the laser current with a frequency of 4 kHz. As in previous work [11,12], the laser was scanned across the well-characterized absorption line 000-101/110-211 at 7299.431 cm-1 (1369.97 nm). The laser light is collimated and directed through the engine combustion chamber. The transmitted light is detected by an InGaAs semiconductor photodiode, converted into a voltage signal with a low-noise transimpedance amplifier (80 MHz bandwidth), subsequently digitized with a 14 bit high-speed A/D converter (100 MSamples/s), and evaluated with in-house LabView software using Eq. (I) and (2).

To evaluate the H_2O absorption line, a polynomial baseline (containing all disturbance information) as well as a Voigt line-shape was fitted to the measured H_2O spectrum. To account for overlapping absorption lines from 7294 cm-1 to 7306cm-1 a multi-line Voigt fit with 21 lines (all stronger than 10^{-23} (cm-1)/(molecule x cm-2)) was applied. The widths of all lines were calculated using HITRAN08 data [18], the measured gas pressure, and the derived temperature from the TPA model. For the target line at 7299.431 cm-1, used to determine the H_2O concentration, we used air-pressure broadening and its temperature dependence, measured by Hunsmann et al. [27].

2.3. Fi,ber-optical interface

The fiber-optical transmitter and receiver had to comply with several requirements:

1. Sealing the launch and collection optics against the hot combustion gases at high pressure (here, $p_{max}=4$ MPa and $T_{max}=2400$ K) and at sub-atmospheric pressures during the intake stroke.

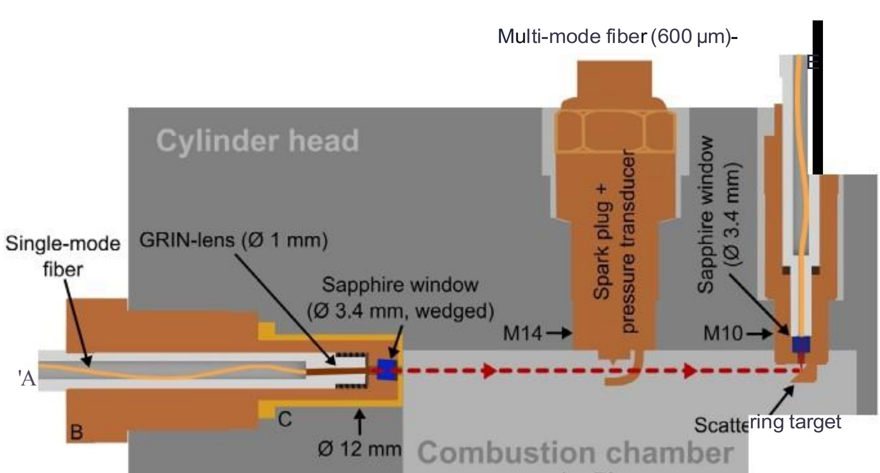

Fig. 3. Schematics of the opto-mechanics of the spectrometer and the fiber-optical interface with fiber transmitter and the 90° receiver with scattering target.

2. Minimizing optical interferences (fringing) of the laser light.
3. Transmitting the laser beam through the combustion chamber at maximized absorption length L to measure a "global" H_2O concentration, despite the new, but unfavorable 90° geometry and small optical access ports, as shown in Fig. 1.
4. Robust, error-tolerant alignment optics insensitive to e.g. beam-steering by density gradients in the gas.
5. Easy assembly/disassembly into/from the engine when occasionally cleaning is required.

Figure 3 shows our new opto-mechanical interface for this challenging scenario. It makes use of ports originally meant for a detection endoscope and the pressure-transducer bore (labels 2 and 6, respectively, in Fig. 1). The light is guided to the transmitter by a single-mode fiber, collimated, and transmitted through a path corresponding to almost the entire cylinder bore onto a scattering target that also enables the 90° bend required in this beam geometry. Close to and mechanically connected with the target a fibered receiver optic is placed, which collects the scattered light and directs it into a multi-mode fiber guiding it to the detection unit. Since the pressure transducer is removed, the standard spark plug (label 3 in Fig. 1) was replaced by a one with an integrated pressure sensor (Kistler BCD27), positioning the ground electrode to avoid obstruction of the laser beam.

The cylindrical, optical transmitter (label A in Fig. 3) holds a gradient-index **(GRIN)** lens with a diameter of 1 mm for collimating the light beam. The second cylinder (B) mounts into the thread of the optical access port in the engine head. It holds a sapphire window (diameter 3.4 mm, thickness 3 mm) mounted at an angle of 3° with a wedge of 2° to avoid optical interferences by light back-reflected at its planar surfaces. The window is fixed and sealed with high-temperature epoxy adhesive, but in addition an outer, thin-shelled cylinder (C) prevents the window from potentially falling into the combustion chamber and damaging the engine if the adhesive fails or the window breaks. The transmitter's outer diameter of 12 mm is given by the port size; a shoulder on that diameter provides pressure sealing, and the front aperture is 1.9 mm in diameter.

The receiver unit consists of two cylinders. The outer one (D) holds the scattering target at an angle of 45°. The brass target has a flat, intentionally poorly-polished surface. It has an area of 35 mm^2 and redirects the light by a semi-diffuse reflection towards the receiving multi-mode fiber. Specular reflection by a highly polished surface might increase the coupling efficiency, but at the cost of a considerably reduced tolerance against alignment errors. Like the transmitter, the receiver is protected from the engine cylinder environment by a sapphire window. The diffuse reflection reduces the coherence length of the laser light such that it is not necessary to wedge or angle the window, which simplifies manufacturing of both window and holder. The inner cylinder *(E)* holds a multi-mode fiber with a core diameter of 600 µm, directly attached to the sapphire window.

For the measurements presented here, about 1% of the light emitted from the single-mode fiber is detected. The rather weak coupling is caused by the geometric constraints and the harsh environment. It is also the reason for using the more powerful DFB laser instead of a weaker vertical-cavity surface-emitting laser (VCSEL), despite the advantages that VCSELs were shown to have at higher gas pressures [11,12].

3. **Results**

A key requirement for *in situ* dTDLAS is the determination and correction of background disturbances like thermal emission from walls or broadband transmissions losses (see Section 2.2). With these corrections several measurements were performed during fired operation and the H_2O concentration was determined at different operating points. The measured H_2O concentration was then compared with the calculated concentration derived from the **EGR** simulation model.

Figure 4 shows - as a function of crank angle - the measured transmission *Tr(t)* of the laser light as well as the background emission (signal offset at the detector) due to thermal emission *E(t)* for a typical single engine cycle after 30 min of fired operation at operating point 2 (OP 2). Here, the transmission was calculated from the measured voltage at the maximum of the triangular ramp signal. The value at -360 crank angle degree (CAD) served as a reference. The offset was

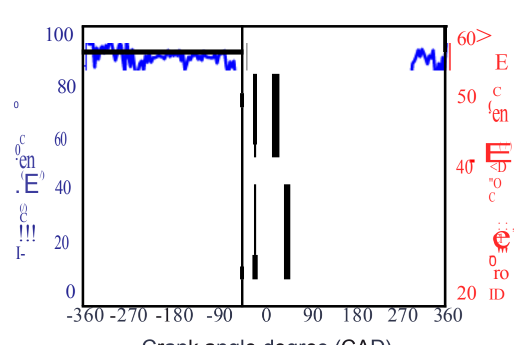

Fig. 4. Measured sensor transmission and background emission during a single fired engine cycle.

derived from the detector signal at the beginning of the ramp, when the laser is switched off. Transmission during the intake and compression stroke before ignition is over 75%. During combustion, transmission decreases rapidly to 5-10% at 60 CAD, potentially due to strong beam steering in the flame front. In the exhaust stroke transmission recovers to more than 90%. This indicates that the period during which useful measurements are possible comprises intake, compression, and exhaust stroke.

The measured offset shows a trend opposite to that of transmission. During intake and compression stroke there is an offset of about 25 mV, very likely due to thermal radiation from the walls (less than 6 mV in the cold engine). After ignition the offset quickly increases to a maximum value of 53 mV due to radiation from the combustion process. In the exhaust stroke the offset decreases back to 25 mV.

To correct for these effects the offset voltage due to background emission is subtracted from the signal and a polynomial baseline is fitted to the signal to correct for fluctuations in the transmission. These two corrections were done for every single measurement. Figure 5 shows two single-shot water-vapor absorption profiles measured at -180 and -100 CAD during fired operation at **OP** 2. The native temporal resolution was 250 µs, corresponding to the laser modulation frequency f_{mod} = 4 kHz. Both signals were low-pass filtered with a moving-average filter over 0.6 µs (corresponding to 0.0065 cm^{-1}) to minimize the effect of detector noise while retaining the molecular spectral information.

The increasing width of the absorption line with increasing pressure can be seen. With increasing pressures the fitting process was more stable when the line width was calculated by using the measured pressure instead of fitting the width as a free parameter. Using this calculated line width, the averaged fitting residual (i.e., the standard deviation of the difference between measured and fitted data) of the scan was determined to be $1\sigma = 1.9 \times 10^{-3}$ fractional absorbance. The 1σ standard deviation of this residual and the peak absorbance was used to derive an optical signal-to-noise ratio (SNR) of 59 (52) at -180 CAD (-100 CAD), corresponding to a H_2O detection limit of 0.074 vol.% (measured H_2O concentration divided by signal-to-noise ratio).

The CAD range in which measurements at all operating points were post-processed was -190 to -100 CAD. Above a certain maximum temporal rate of change in pressure and temperature, depending on several parameters *e.g.,* temporal resolution, engine speed, concentration, *etc.,* the line-shape essentially cannot be assumed anymore to be constant during a single scan [11] so that systematic errors became unacceptable. Faster scans with the DFB laser, however, reduce the effective

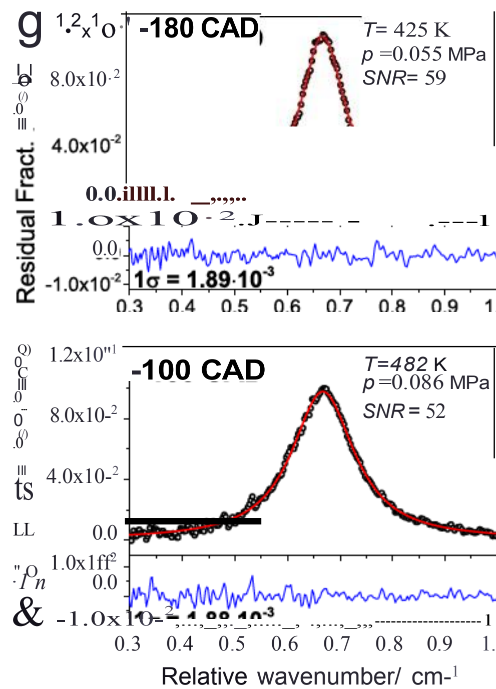

Fig. 5. Two typical H_2O absorption profiles (black points: measured data, red lines: fitted Voigt profiles) in fired operation (OP 2). Temperature and pressure were obtained from simulations and measurements and used as input parameter to the fit. (For interpretation of the references to colour in this figure legend, the reader is referred to the web version of this article.)

scan range, which also reduces the fit accuracy. This effect limited the maximum pressure range of the TDL spectrometer with the current DFB laser and data evaluation to 0.2 MPa. At some operating points, a broader CAD range could be evaluated, but to compare all measurements a common CAD range was chosen. Figure 6 shows the measured H_2O concentrations for a typical, single engine cycle each at OP 1-4 (the load sweep). The average H_2O concentration decreases with increasing load from 5.0 vol.% at 25 Nm to 3.4 vol.% at 100 Nm. This trend qualitatively validates sensor function since greater intake-valve lift and longer valve overlap at higher load (see Table 1) should yield better exhaust-gas purging.

These measured H_2O concentrations are compared with simulations for the residual gas fraction. With known fuel composition and intake air humidity (0.61 vol.%) and assuming complete combustion, the residual gas fraction can be converted to H_2O concentration and vice versa. The comparison between the averaged H_2O concentrations of 50 engine cycles is shown in Fig. 7 for load variation (top, OP 1-4) and speed variation (bottom, OP 5-8). For better clarity the data from dTDLAS measurement and the residual gas model have been shifted slightly against each other in

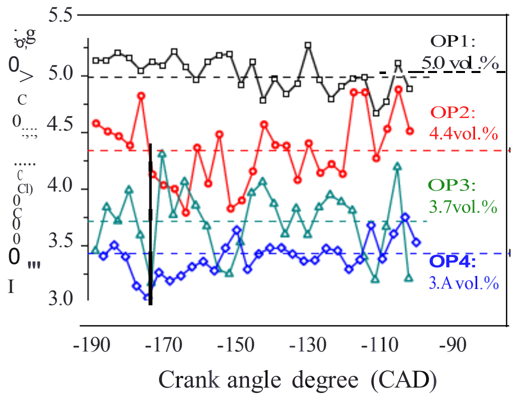

Fig. 6. Measured H_2O concentration from -190 to -100 CAD during single engine cycles at different operating points (OP 1-4). The intake air contained 0.61 vol.% H2O,

load or speed, as applicable. The relative uncertainties of the dTDLAS measurements werecalculated according to the metrological guide to the expression of uncertainty in measurement (GUM) [28] to 7.5% (for a coverage factor: $k = 1$). The largest uncertainty contribution

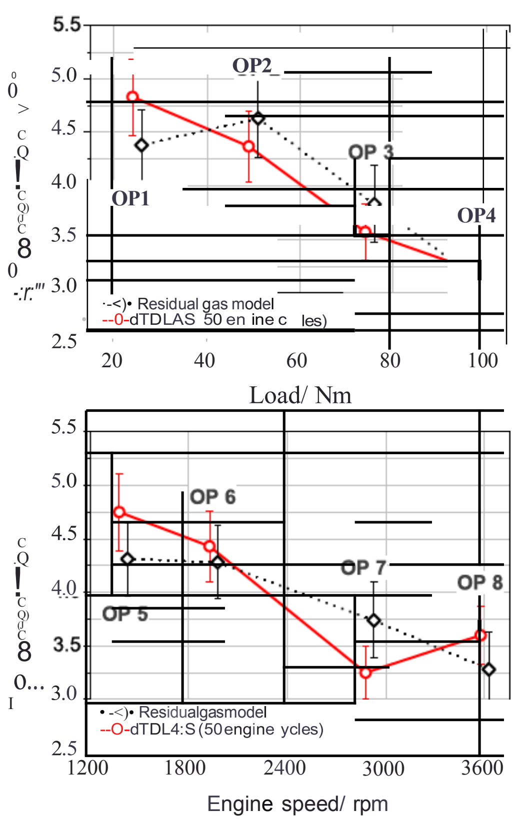

Fig. 7. Comparison of measured H2O concentrations (dTDLAS) at various OPs with concentrations derived from the residual gas model.

(60%) originated from the temperature uncertainty, about 15 **K** over the crank-angle range evaluated here. In the quasi-dimensional three-pressure analysis providing this in-cylinder temperature, the main source of uncertainty is the duration of valve overlap read from the engine control unit (±4 CAD), yielding 12 K uncertainty, with further minor contributions from injected fuel mass and fuel/air ratio. The uncertainties of the residual gas model were estimated by varying the main input parameters within their measurement uncertainty, valve timing (±2 CAD), exhaust temperature (±50 K), and intake-to-exhaust pressure difference (±o.Dl MPa). The cycle-to-cycle variations of temperature and pressure within each operating point were also considered (one standard deviation). Conversion from residual gas content to H_2O concentration (and vice versa) is associated with additional uncertainties, most significantly the excess air-fuel ratio l measured by the oxygen sensor. Typical uncertainties for commercial sensors like the one used here are ±4%, resulting in an additional uncertainty between 0.09 and 0.14 vol.% H_2O, depending on the operating point.

Figure 7 shows that simulation and measurements agreewithin their uncertainties. For all operating points the average difference between measurement and simulation is about 8% with the best agreement at OP 6 with a difference of only 3.3%. (In fact, especially in the "outliers" like OP 1, 5, and 7 the agreement is *better* ifwe ignore the sensor data and set l = 1.00, indicating that the oxygen sensor may be themost significant error contribution.) We may thus conclude that given its simplicity the residual gas model works quite well.

4. Conclusions

A new dTDLAS spectrometer was developed which allowed the first calibration-free, absolute measurement of H_2O concentrations along a path through the combustion chamber of a near-production internal combustion (IC) engine. The H_2O concentration serves as a proxy for the amount of residual gas in the cylinder after gas exchange. The four-cylinder inline production engine was equipped with two optical accesses. Because of the positions of the optical accesses they could not be used as-is for a line-of-sight method like dTDLAS. Therefore, a new, angled fiber-optical interface was developed that uses one optical access and the bore for the pressure transducer together with a scattering target inside the cylinder. The scattering target allows turning the laser beam by an angle of 90°, which enables the usage of the non-collinear ports, while considerably increasing alignment tolerance. The interface can be used with small ports (<12 mm). Especially the scattering target and the windows proved to be insensitive to fouling and able to easily withstand hours of fired operations.

In contrast to other techniques applied for in-cylinder gas analysis, dTDLAS can be performed without calibration. It was already validated in a single-cylinder research engine [11,12]. Also strong and rapid transmission and emission changes, caused by the combustion process, can be monitored too and effectively corrected for. Residual gas content was evaluated during the compression stroke from -190 to -100 CAD. With a signal-to-noise ratio of over 50 and an optical resolution (lo-) of 1.9 x 10^{-3} fractional absorbance, a detection limit of 0.074 vol.% H_2O could be achieved.

Several operating points with variations in engine speed (up to 3650 rpm) and loads (up to 100 Nm) were used to induce changes in the residual gas content. From an engine model the residual gas content and thus the H_2O concentration were calculated and the latter was compared with the dTDLAS measurements. Within the uncertainty of the dTDLAS measurement (7.5%) and the residual gas model (6.8-12%) good agreement between measurement and simulation could be found. Since the laser-absorption method had already been validated under engine conditions, albeit in motored operation in a research engine, this comparison in fired operation shows that dTDLAS is a useful tool for validating or improving more complex engine models in terms of residual gas content, a variable that cannot be checked directly by other means.

Further measurements will be performed to extend the number of operating points for the comparison with the residual gas model. The model is simple enough that, together with a zero-dimensional model of compression, it could be integrated into the dTDLAS evaluation itself to augment that diagnostic with the needed input parameter temperature in an iterative fashion. Measurements with a another laser type (VCSEL) are planned that allow an extension of the measurement to the entire compression stroke, with an additional increase in the temporal resolution. Also, a single-port sensor is under development, which will enable measurements in any cylinder of a multi-cylinder engine, making this technique more widely applicable.

Acknowledgments

The IGF Project 15970 N of the research asso-c1at10n Forschungskuratorium Maschinenbau e.V. - FKM, Lyoner StraBe 18, 60528 Frankfurt, was funded via the *AiF* within the Industrielle Gemeinschaftsforschung und -entwicklung (IGF) by the Federal Ministry of Economy. The authors thank C. Gessenhardt and M. Goschiitz from the IVG for construction and help with operation, respectively, of the engine test cell.

References

[I] A.A. Quader, R.F. Majkowski, SAE Paper No. 1999-01-11, 1999.

(2] T. Toda, H. Nohira, K. Kobashi, SAE Paper No. 760765, 1976.

[3] M.C. Weik!, F. Beyrau, A. Leipertz, *Appl Opt.* 45 (2006) 3646-3651.

(4] DA. Rothamer, J.A. Snyder, R.K. Hanson, R.R. Steeper, *Appl. Phys. B* 99 (2009) 371-384.

(5] E. Tomita, N. Kawahara, M. Shigenaga, A. Nishiyama, R.W. Dibble, *Meas. Sci. Technol* 14 (2003) 1350-1356.

[6] D.W. Mattison, J.B. Jeffries, R.K. Hanson, R.R. Steeper, S. De Zilwa, J.E. Dec, M. Sjoberg, W. Hwang, *Proc. Combust. Inst.* 31 (2007) 791-798.

[7] G.B. Rieker, H. Li, X. Liu, J.T.C. Liu, J.B. Jeffries, R.K. Hanson, M.G. Allen, S.D. Wehe, P.A. Mulhall, H.S. Kindle, A. Kakuho, K.R. Sholes, T. Matsuura, S. Takatani, *Proc. Combust. Inst.* 31 (2007) 3041-3049.

[8] K. Akihiko, K.R. Sholes, H. Yutaka, T. Shohei, U. Tomonori, R.K. Hanson, J.B. Jeffries, M.G. Allen, SAE Paper No. 2007-01-06, 2007.

[9] M. Cundy, T. Schuch!, 0. Thiele, V. Sick, *Appl. Opt.* 48 (2009) 94-104.

(10] K.D. Rein, S.T. Sanders, R.J. Bartula, SAE Paper No. 2009-01-08, 2009.

(11] 0. Witzel, A. Klein, C. Meffert, S. Wagner, S. Kaiser, C. Schulz, V. Ebert, *Opt. Express* 21 (2013) 19951.

(12] 0. Witzel, A. Klein, S. Wagner, C. Meffert, C. Schulz, V. Ebert, *Appl. Phys. B* 109 (2012) 521-532.

(13] A. Farooq, J.B. Jeffries, R.K. Hanson, *Meas. Sci. Technol* 19 (2008) 075604.

(14] H. Teichert, T. Fernholz, V. Ebert, *Appl. Opt.* 42 (2003) 2043-2051.

(15] M.E. Webber, J. Wang, S.T. Sanders, D.S. Baer, R.K. Hanson, *Proc. Combust. Inst.* 28 (2000) 407-413.

(16] C. Schulz, A. Dreizler, V. Ebert, J. Wolfrum, *Combustion diagnostics,* in: C. Tropea, A.L. Yarin, J.F. Foss (Eds.), *Springer Handbook of Experimental Fluid Mechanics,* Springer, Berlin, Heidelberg, 2007, pp. 1241-1315.

(17] B. Buchholz, B. Killmreich, H. Smit, V. Ebert, *Appl Phys. B* 110 (2013) 249-262.

(18] L.S. Rothman et al., *J. Quall/. Spectrosc. Radial. Transf* 110 (2009) 533-572.

(19] A. Grosch, H. Wackerbarth, 0. Thiele, T. Berg, L. Beckmann, *J. Quant. Spectrosc. Radiat. Trans/* 133 (2014) 106-116.

(20] C. Gessenhardt, F.P. Zimmermann, C. Schulz, R. Reichle, C. Pruss, Osten, SAE Paper No. 2009-01-06, 2009.

(21] R. Reichle, C. Pruss, C. Gessenhardt, C. Schulz, W. Osten, *Appl Opt.* 51 (2012) 1982-1996.

(22] C. Gessenhardt, Ph.D thesis, University of Duisburg-Essen, Germany, 2013.

(23] M. Bargende, U. Kohler, F. Schwarz, U. Spicher, Entwicklung eines allgemeingiiltigen Restgasmodells fiir Verbrennungsmotoren, Forschungsvereinigung Verbrennungskraftmaschinen (FVV), Report No. 740.

(24] V. Ebert, H. Teichert, P. Strauch, T. Kolb, H. Seifert, J. Wolfrum, *Proc. Comhust. Inst.* 30 (2005) 1611-1618.

(25] H.E. Schlosser, J. Wolfrum, V. Ebert, B.A. Williams, R.S. Sheinson, J.W. Fleming, *Proc. Comb. Inst.* 29 (2002) 353-360.

(26) V. Ebert, T. Fernholz, C. Giesemann, H. Pitz, H. Teichert, J. Wolfrum, H. Jaritz, *Proc. Combust. Inst.* 28 (2000) 423-430.
(27) S. Hunsmann, S. Wagner, H. Saathoff, O. Mohler, U. Schurath, V. Ebert, VDI, Report No. 1959, 2006, pp. 149-164.
(28) JCGM 100:2008, Evaluation of measurement data - Guide to the Expression of Uncertainty in Measurement, GUM 1995 with minor corrections, ISO IEC Guide 98-3, 2008. <http//www.bipm.org/utils/common/documents/jcgm/JCGM_100_2008_E.pdf>.